

Are Homologous Radio Bursts Driven by Solar Post-Flare Loops? *

Min Wang¹, Rui-Xiang Xie¹, Yi-Hua Yan² and Yu-Ying Liu²

¹ National Astronomical Observatories/Yunnan Observatory, Chinese Academy of Sciences, Kunming 650011; wm@ynao.ac.cn

² National Astronomical Observatories, Chinese Academy of Sciences, Beijing 100012

Received 2006 August 2; accepted 2006 December 28

Abstract Three particularly complex radio bursts (2001 October 19, 2001 April 10 and 2003 October 26) obtained with the spectrometers (0.65–7.6 GHz) at the National Astronomical Observatories, Chinese Academy of Sciences (NAOC, Beijing and Yunnan) and other instruments (NoRH, TRACE and SXT) are presented. They each have two groups of peaks occurring in different frequency ranges (broad-band microwave and narrow-band decimeter wavelengths). We stress that the second group of burst peaks that occurred in the late phase of the flares and associated with post-flare loops may be homologous radio bursts. We think that they are driven by the post-flare loops. In contrast to the time profiles of the radio bursts and the images of coronal magnetic polarities, we are able to find that the three events are caused by the active regions including main single-bipole magnetic structures, which are associated with multipole magnetic structures during the flare evolutions. In particular, we point out that the later decimetric radio bursts are possibly the radio counterparts of the homologous flares (called “homologous radio bursts” by us), which are also driven by the single-bipole magnetic structures. By examining the evolutions of the magnetic polarities of sources (17 GHz), we could presume that the drivers of the homologous radio bursts are new and/or recurring appearances/disappearances of the magnetic polarities of radio sources, and that the triggers are the magnetic reconnections of single-bipole configurations.

Key words: Sun: radio radiation — Sun: magnetic fields

1 INTRODUCTION

Post-flare loops are the most persistent features associated with the classic large two-ribbon flares. These loop systems rise slowly into the corona during the main phase (corresponding to the decaying phase of radio burst) of the flare. The ascent velocity decreases with height from about 10–20 km s⁻¹ at the beginning to a fraction of a km s⁻¹ when they are finally observed in SXR (Soft X-ray) at great heights (Pneuman 1981). Priest (1981) indicated that a two-ribbon flare contains two stages: the initial filament eruption and the formation of post-flare loops. When a filament erupts and drags the magnetic field lines with it, an open current sheet configuration is formed. The open field lines then close back down and create post-flare loops as the flare develops. Most reliable and extensive observations of this type of two-ribbon flares were taken early in the 1970s (Pneuman 1981).

The Solar Flare Workshop have exhibited some classical post-flare loop systems (Moore et al. 1980). However, it is still a matter of discussion as to what produces the post-flare loops: whether post-flare loops result from the closing up of an open configuration or the spreading of a disturbance through a closed one; or whether post-flare loops produce homologous flares or new flares. Thus, more observational information on the detailed magnetic structures and multiband around post-flare loops are needed.

* Supported by the National Natural Science Foundation of China.

The magnetic configuration of solar flare is essential to the study of energy storage, energy release and particle acceleration in flares. It has been found that interaction of magnetic bipoles is a key ingredient in causing flares (Mandrini et al. 1991; Démoulin et al. 1993; Machado et al. 1998). The flare models with presumed energy release sites near (or above) the loop top were essentially provided and considered in some theoretical and observational models (Masuda et al. 1994; Mandrini et al. 1991; Hanaoka 1997; Nishio et al. 1997; Aschwanden et al. 1999), but the observational verification is still needed. It has been known that different flares have different energy outputs and distributions over the different frequency bands, and different evolution time scales. Thus a unified theoretical interpretation of solar flares looks impossible. Different types of flares have to be explained as resulting from basically different magnetic configurations and physical mechanisms.

We observed three radio bursts associated with two-ribbon flares on 2001 October 19, 2001 April 10, and 2003 October 26. In particular, they contained two groups of radio emission peaks occurring respectively at microwave and decimeter wavelengths. The decimetric radio peak occurred in the late phase of the flare. They may be the radio counterparts (here, we call them “homologous radio bursts”) of another kind of homologous flares caused by post-flare loops. The three bursts are analyzed in this paper using data obtained by the radio spectrometers at the National Astronomical Observatories of China (NAOC), the Nobeyama Radio Heliograph (NoRH, Nakajima et al. 1994), the Michelson Doppler Imager (MDI), the Transition Region and Coronal Explorer (TRACE), and the Yohkoh/SXT. The NoRH images especially allowed us to make a better comprehensive analysis of the magnetic configurations. We aim in this work to gain an insight on the magnetic topologies of these events (Green et al. 2002) that determines whether a decimetric radio burst is likely to be related to a post-flare loop.

Section 2 of this paper describes the instruments and observational characteristics of the whole radio bursts, as well as the evolutions of radio sources reflecting the coronal magnetic structures. Section 3 analyzes the magnetic configurations of the two separate groups of radio emission peaks, the correlation between the burst peaks and the heights of expanding post-flare loops, the magnetic configurations and the radio emissions of fast time structures (FTSs) associated with the homologous radio bursts. Sections 4 and 5 give, respectively, a discussion and a summary of the occurrence and the process occurring in the homologous radio bursts.

2 OBSERVATIONS AND DATA PROCESSING

2.1 Instruments

A decimetric radio spectrometer in the range of 1.0 – 2.0 GHz and a microwave spectrometer in the range of 2.6 – 3.8 GHz and 5.2 – 7.6 GHz at the NAOC have come into operation since 1993, 1996 and 1999, respectively (Ji et al. 1997; Ji et al. 2000). In addition, a spectrometer (0.65 – 1.5 GHz) at Yunnan Observatory has been put into operation since July 2000. It uses a 10-m diameter antenna, with a spectral resolution of about 1.4 MHz and time resolution of 8 ms. The dynamic range is better than 10 db. The flux and circular polarization are recorded digitally, and the degree of polarization has an accuracy better than 10%.

2.2 Characteristics of Radio Observations

Three complex radio bursts (2001 October 19, 2001 April 10, and 2003 October 26) were observed with the four spectrometers. All four are each associated with a two-ribbon flare, of importance 2B/X1.6, 3B/X2.3 and 3B/X1.2, and located at N14 W22 (AR 9611), S23 W09 (AR 9415), and S17 E42 (AR 10486), respectively. Figures 1–3 show the time profiles of the three bursts for the selected frequencies of the four spectrometers. We find that the three bursts have some common morphological features. In the radio time profiles of the radio bursts, we can clearly distinguish two groups of burst peaks (i.e., the so-called homologous radio bursts) with the quiet time intervals of the order of 2, 8 and 5 minutes, and the peak-peak intervals of the order of 25, 45 and 70 minutes. Based on these observational characteristics the two separate radio bursts are similar to the homologous flares as defined in Woodgate et al. (1984):

(a) The members of homologous radio bursts have the same main magnetic polarities of the radio sources at 17 GHz (they would be corresponding to the main footpoints of the flares), see figures 4b and 5d in Wang et al. (2005), and Figures 4c and 4l in this paper;

(b) The separate radio bursts show similar dynamic spectra and morphological appearances (see Figs. 1, 2 and 3);

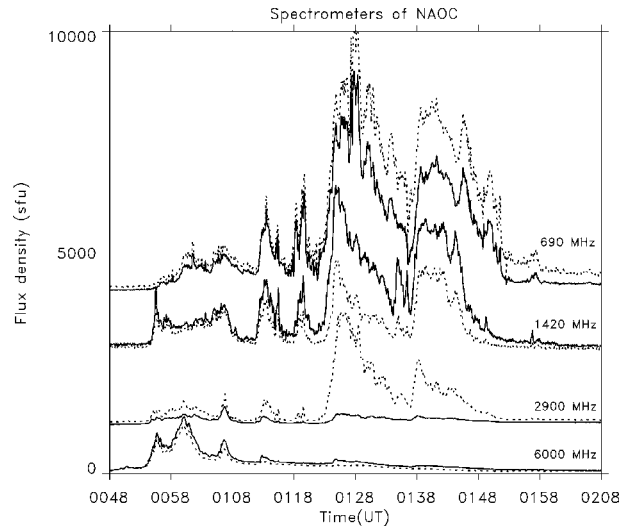


Fig. 1 Spectrogram (time profiles) of radio bursts on 2001 October 19 at selected frequencies. Dashed lines for the right polarization, and solid lines, the left polarization.

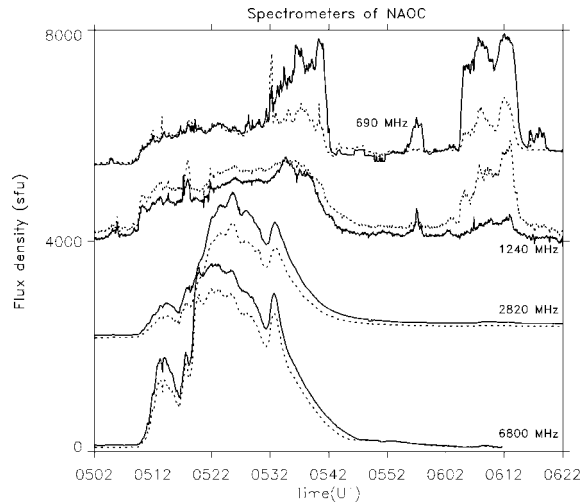


Fig. 2 Spectrogram (time profiles) of radio bursts on 2001 April 10 at selected frequencies. Dashed lines for the right polarization, and solid lines, the left polarization.

(c) There is a time interval between the two homologous flares, but the types of homologous flares classified by Martres (1989) showed that the intervals of time separation are in hours, while the time separations of the radio bursts in the present work are in minutes, therefore, they can be treated as homology-like radio flares.

Moreover, there are various FTSs accompanying the continuum emissions, i.e., normal and reverse drifting type III bursts, no drifting and slowly drifting structures (see Wang et al. 2005). Most of these occurred in the impulsive phase of the radio bursts. In particular, we should mention that the coronal magnetic structures of the three events varied strongly during the impulsive phase of the microwave radio bursts. This could be a hint that the radio emissions depend on the varying magnetic configurations (Aschwanden 2002).

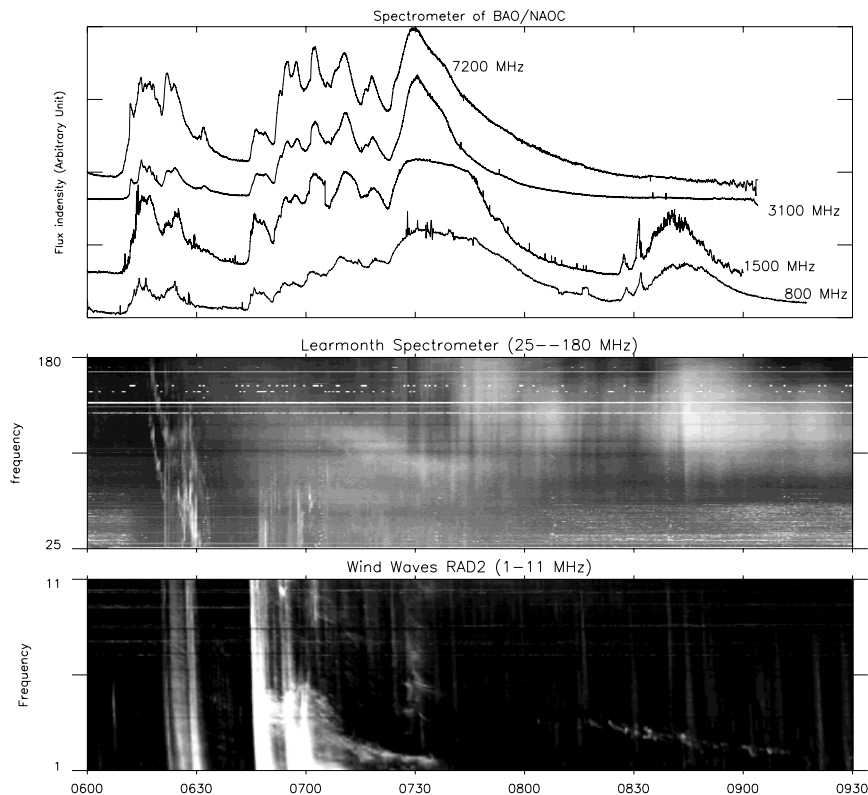


Fig. 3 Top panel: Spectrogram (time profiles) of radio bursts on 2003 October 26 at selected frequencies; Middle: Spectrum of Learmonth; Bottom: Spectrum obtained by spectrograph WAVES on board spacecraft WIND.

2.3 Evolutions of Coronal Magnetic Structures Related to the Radio Bursts

All three events showed very complex magnetic structures as the flares developed. There were newly appearing/disappearing radio sources as well as a preexisting radio source. The NoRH images at 17 GHz (I and V) of the radio bursts on 2001 October 19 and 2003 October 26 are shown in Figures 4 and 5, respectively. The NoRH images of 2001 April 10 event can be seen in Wang et al. (2005). From these images we can see how the coronal magnetic polarities at 17 GHz evolved (they could represent the foot points of magnetic flux loops) during the bursts.

(1) The 2001 October 19 Event Figures 4(a) and 4(b) show the preexisting magnetic unipole (positive V) and a gradual radio source superimposed on the unipole (marked by 'A') before the beginning of the radio burst. This would be the building-up process of the flare preheating (Kundu 1983).

Figure 4c shows a newly appeared magnetic pole (negative V , marked by 'B') and a another radio source (marked 'A''') above the newly appearing pole, before the beginning of the radio burst. Two opposite polarities may be reconnected to form an inverted 'Y-type' structure, leading to the two-ribbon flare related to the broad-band radio burst.

Figure 4d shows another two newly appeared magnetic poles (positive V , marked by 'C' and 'D'). 'D' is between the two original poles, 'A' and 'B'. At this time a quadrupolar structure appeared.

Figure 4e shows the two newly appeared positive poles ('C' and 'D' see Fig. 4d) to be disappearing. However, the positive pole 'D' has changed into a negative pole 'E'. Figure 4f shows a disappearing negative pole 'E'; Figure 4g shows again a reappearing negative pole 'E'; Figure 4h shows the same structure as Figure 4f; Figure 4i shows the only positive pole 'A'; Figures 4j and 4k show a reappearing negative pole 'E';

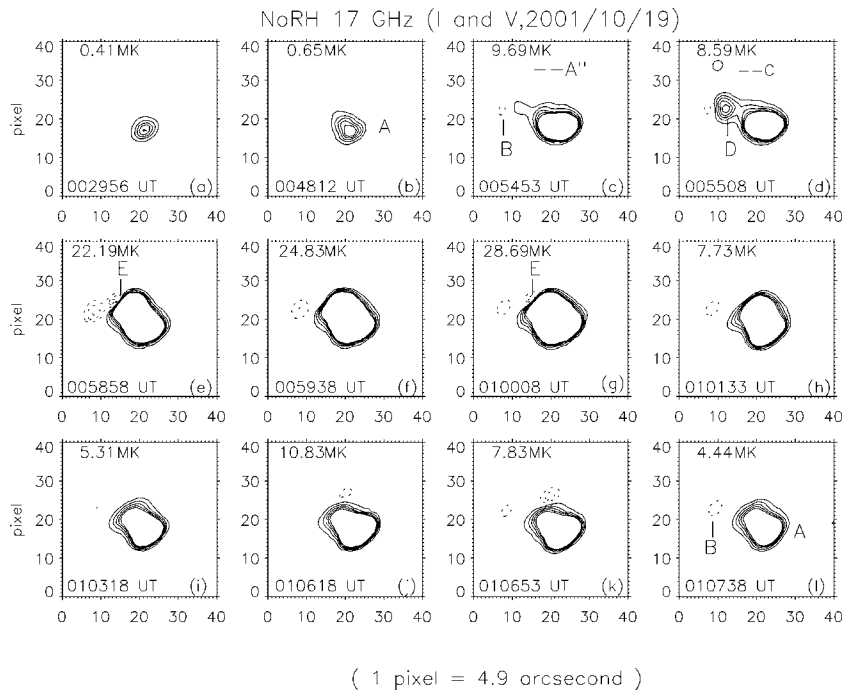


Fig. 4 Evolution of the NoRH radio sources at 17GHz of the event of 2001 October 19. The characters across the top of each image are the maximum values of Stokes *I*. The solid and dashed heavy contours represent positive and negative Stokes *V*; the light contours, Stokes *I*.

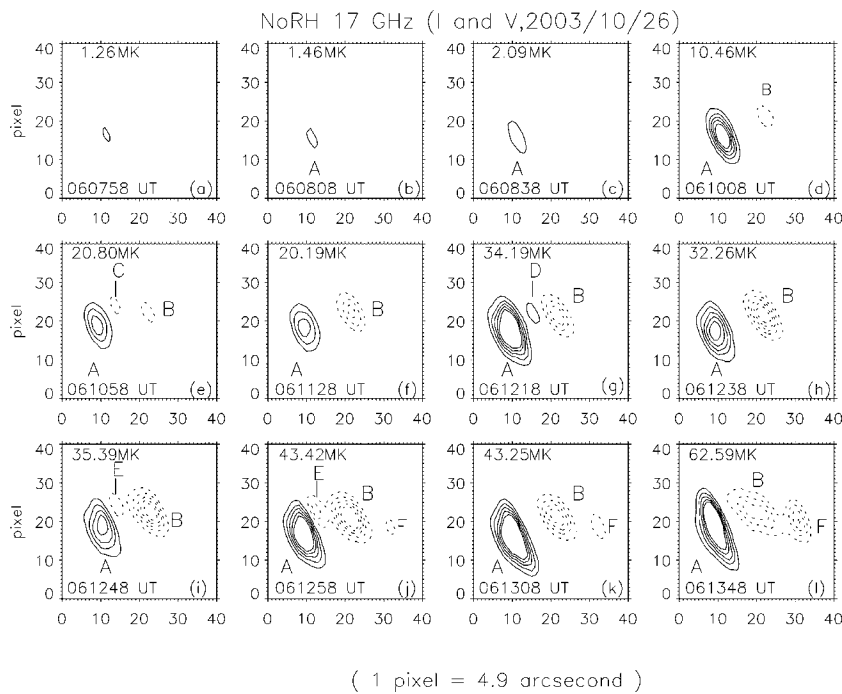


Fig. 5 Evolution of NoRH radio sources of the event of 2003 October 26 at 17GHz. The light contours represent the Stokes *I*, the heavy solid and dotted contours represent positive and negative Stokes *V*. The characters across the top of each images are the maximum values of Stokes *I*.

Figure 4l shows the finally two opposite polarities 'A' and 'B', which would be the magnetic configuration resulting in the late phase decimetric homologous radio burst occurring near the apex of the post-flare loops.

(2) The 2003 October 26 Event The magnetic polarity evolution in this case is similar to that of the 2001 October 19 and 2001 April 10 events. It has available only data of magnetic polarities for the time of impulsive phase of the burst.

Figures 5a, 5b and 5c show the preexisting magnetic unipole (positive V) and a gradual radio sources superimposed on the unipole (marked by 'A') before the beginning of the radio burst. This reflects the process of flare preheating (Kundu 1983).

Figure 5d shows a newly appearing magnetic pole (negative V , marked by 'B') and another radio source near the newly appearing pole, before the beginning of the radio burst. Two opposite polarities may be reconnected to form an inverted 'Y-type' structure leading to the two-ribbon flare related to the broad-band radio burst.

Figure 5e shows another newly appearing magnetic pole (negative V , marked by 'C'). 'C' lies between the two original poles. At this time a tripolar structure appears.

Figure 5f shows a newly appeared negative pole 'C', which again disappears;

Figure 5g shows a newly appearing positive pole (marked by 'D') to lie between the 'A' and 'B';

Figure 5h shows the newly appearing positive pole 'D' again to be disappearing;

Figure 5i shows a positive pole 'D' (see Fig. 5g) changing into a negative pole 'E';

Figure 5j shows again a newly appearing negative pole 'F';

Figure 5k shows the newly appeared negative pole 'E' to be disappearing;

Figure 5l shows the finally two opposite polarities. At this time the two negative poles 'B' and 'F' have joined together. This magnetic configuration would result in the late phase decimetric homologous radio burst occurring near the apex of the post-flare loops.

2.4 Appearances of the Post-Flare Loops

When a flare occurs, SXR observations typically show a sudden formation of bright loops. In particular, in the gradual or decay phases of the flare definite post-flare loops can appear, in which we can see expanding SXR loops in the late phase of the flare, e.g., the event on 2001 October 19 (Fig. 7). The SXR loops first appeared near the footpoints in the beginning of then flares, then grew and expanded. Moreover, the EUV emission also showed loop-system consisting of many loops in the late phase of flares. When the SXR observation is completely saturated, we can also see multiple EUV post-flare loops, e.g., the events on 2001 April 10 and 2003 October 26 (Figs. 6 and 8). The radio loops should be inferred according to the different polarities of the microwave polarization. In this paper all three events included a main single-bipole evolving to a four-pole structure as the flares developed, but the radio homologous bursts were caused by the main bipole structure (e.g., fig. 5d in Wang et al. 2005, and Fig. 4l in the present paper).

3 ANALYSIS

3.1 Magnetic Configurations of the Homologous Radio Bursts

A recent interest (Hudson et al. 2004) is using flare observations to confirm the connectivity and to infer the sites of energy storage and release. That magnetic energy stored slowly in the corona can be released suddenly in a flare is in agreement with the thinking of most researchers. The geometries and topologies of coronal magnetic fields could be inferred by watching the evolution of a complex radio (17 GHz) source. In theoretical work, there has now been convincing evidence in the late phase of eruptive flares (two-ribbon flares), i.e., the large-scale reconnection pictures presented by CSHKP models (Aschwanden 2002; Priest & Forbes 2002; Hudson et al. 2004). Here we have observed three broad-band radio bursts with two separate groups of burst peaks in microwave and decimeter wavelengths, and we term the later decimetric bursts as homologous radio bursts. In our analysis of the events the conditions of homologous pre-burst are not re-formed after the first bursts by the emerging flux in the manner indicated by Ranns et al. (2000). These homologous bursts are repeating flare activities, which are triggered by continual flux emerging or submerging (manifested as the appearance or disappearance of magnetic poles of radio sources, see figs. 4 and 5 in Wang et al. 2005; Fig. 4 in this paper). It may include a main single-bipole magnetic structure evolution model (Zhang & Wang 2002; Pneuman 1981), which involves continual magnetic shearing or twisting (Ranns et al. 2000). As the magnetic structures evolve, newly emerged or submerged fluxes reflect

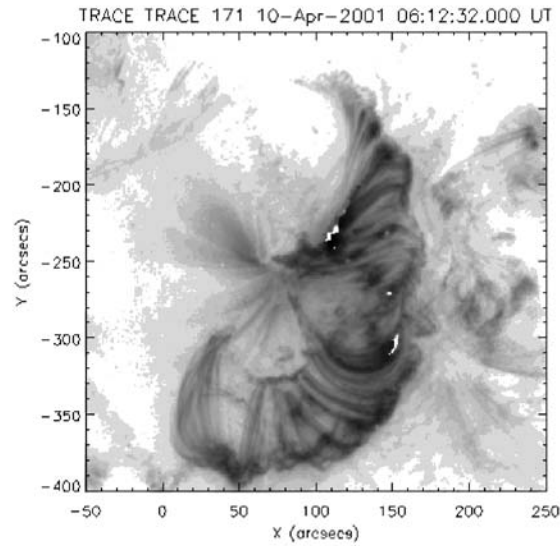


Fig. 6 Post-flare loop-like structures observed by TRACE 171 Å on 2001 April 10.

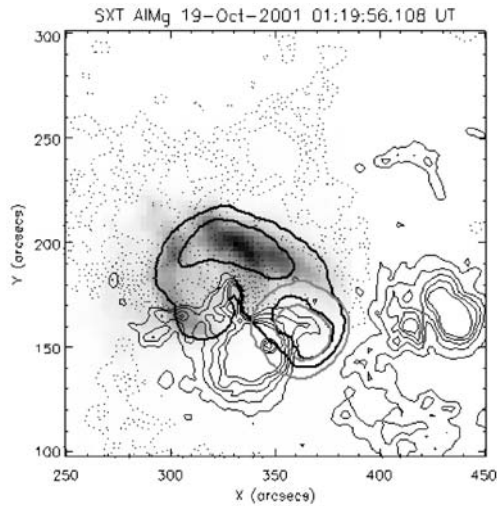


Fig. 7 Post-flare loop-like structures observed by SXT (grey scale image) on 2001 October 19. The black solid and light contours are, respectively, I and $V(+)$ of NoRH (17 GHz). The background (contours) is MDI, with solid (dotted) thin lines for positive (negative) values.

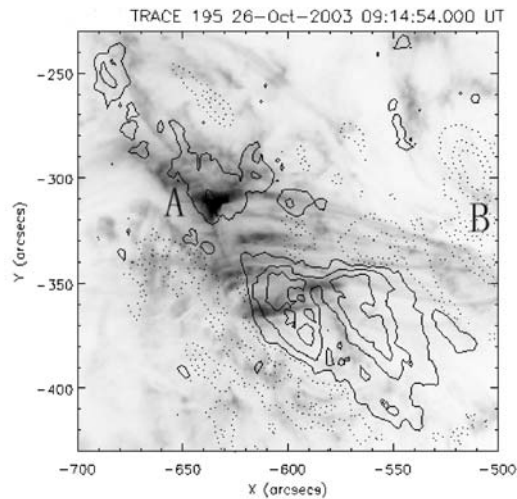


Fig. 8 Post-flare loop-like structures (grey scale image) observed by TRACE 195 Å on 2003 October 26. The background (contours) is MDI, with solid (dotted) lines for positive (negative) values. A and B mark the positions of the footpoints.

the manifestations of the tripolar or quadrupolar magnetic structures (see Figs. 4 and 5). These complex radio bursts (including the homologous bursts) are the results of evolution of multiple magnetic structures (Priest 1981).

According to the evolving images (Figs. 4 and 5) of magnetic polarity, we can presume that there are single loop (e.g., bipole in Figs. 4c and 5d), double-loop (e.g., tripole or quadrupole in Figs. 4d, 4e, 4g, 4k and 5e, 5g, 5i-5l) magnetic configurations with possible 'three-legged' structure (Hanaoka 1997), and the

later multi-loop (e.g., resulting from the quadrupole in Figs. 4d and 5j) magnetic reconnections during the flare evolutions (Aschwanden et al. 1999; Nishio et al. 1997; Hanaoka 1997; Aschwanden 2002).

It is known that a large variety of radio emission types arise from a complex topology of acceleration regions and magnetic configurations. However, the preexisting and newly appeared magnetic polar regions are the essence to produce radio flares and microflares (i.e., radio bursts and radio FTSs) (Martens & Kuin 1989). A single bipolar loop is the outcome of an oppositely directed bipolar reconnection process. Particularly, in our cases, bipolar regions with opposite magnetic fields occurred at the beginning and the late phase of the flares (e.g., Figs. 4c and 4l). This means that a single bipolar loop may exist on two occasions during the production of a two-ribbon flare. The first part of radio bursts (microwave broad-band bursts) seem to involve the energy release sites at the lower heights (foot points of the loop or the low loop of initial disturbance), the second part (e.g., the later decimetric homologous radio bursts) are near the top of post-flare loops. Therefore, magnetic configurations must be varied applying to the later homologous bursts during the flares.

Conceivably, the microwave broad-band and the decimetric narrow-band homologous bursts are caused by the type of bipolar flare model (e.g., in Figs. 4c and 4l), termed inverted ‘Y-type’ structure (Aschwanden 2002; Masuda et al. 1994). The magnetic field topology that we derived from the observations could be similar to the CSHKP model (Carmichael 1964; Sturrock 1966; Hirayama 1974; Kopp & Pneuman 1976). The antiparallel magnetic fields are supposed to be associated with the rising ‘Y-type’ reconnection point that explains the post-flare loops rising with time (Masuda et al. 1995). Our observations of the homologous radio bursts support the model of large-scale reconnection near the top of expanding post-flare loops. This model involves a dissipative process that opens up the magnetic field of the active region. This process allows the field to reform and to release energy into the cusped arcade structure. It is consistent with a quasi-open inverted ‘Y-type’ configuration (Priest & Forbes 2002; Aschwanden 2002; Masuda et al. 1994, 1995).

3.2 Heights of Post-Flare Loops Producing the Homologous Radio Bursts

For obtaining the height of the post-flare loops corresponding to the decimetric bursts, we assume that the magnetic field of the active region is a dipole field below the photosphere at depth d , and the relation between the height above the photosphere h and the frequency f is (Takakura & Scalise 1970; Fu et al. 1985),

$$h = d[(5.6B_0/f)^{1/3} - 1], \quad (1)$$

where B_0 is the magnetic field strength at the photosphere. Assuming $B_0 = 3000$ G, $d = 3.5 \times 10^4$ km in Equation (1), for the expanding upward frequencies (around 2.9, 2.0 and 1.5 GHz in the three events) of the post-flare loop, from the Equation (1) we obtain the expanding loop heights to be 2.9, 2.6 and 1.5×10^4 km, respectively. Assuming the expanding upward velocity of the post-flare loops average 10 km s^{-1} , then the rising heights h are between $2 - 4 \times 10^4$ km, when the times of the decimetric bursts after the microwave bursts peak are of the order of 20, 40 and 56 minutes, respectively. This is basically consistent with the above computing values.

In the impulsive phase of two-ribbon flares the magnetic field lines are dragged upward by the rising filament (or other hot material). In the main phase if an open field is produced, then it will slowly close up back toward a potential structure. The cusp point of an inverted ‘Y-type’ magnetic configuration slowly rises when successive field lines close up. This process can create the expanding post-flare loops (Priest 1981). When the upward moving loops reach the heights corresponding to the short decimeter wavelengths (e.g., 2.9, 2.0 and 1.5 GHz), near the loop tops, radio sources form again (Priest 1981; de La Beaujardière et al. 1995), which could radiate the homologous radio bursts.

3.3 Formations of Radio FTSs

In this paper three radio bursts are associated with FTSs, which are produced during the explosive coalescence process (Tajima et al. 1987). It is generally agreed that the FTS indicate the acceleration of energetic electrons from small magnetic structure in the form of nonthermal emission, while the gradual component of continuum represents energy release from larger magnetic structures through heating (Gopalswamy et al. 1997; Parker 1988). In ‘Y-type’ magnetic configuration associated multipole can occur both long lifetime bursts (two-ribbon flares) and various other active phenomena, such as the FTSs (Hanaoka 1997; Wang et

al. 2005). In addition, we also suggest that the later tripole (e.g., Fig. 4e) may form a ‘three-legged’ structure with two loops. This structure could also produce emissions of FTSs (Hanaoka 1997). The FTSs can be interpreted as follows: When the current sheet forms during the reconnection of two opposite magnetic fields, the resulting anomalous resistivity causes the current sheet to expand rapidly. An induced electric field is therefore generated, which forces the electrons in the current sheet to behave in a runaway manner and/or to generate high-frequency turbulence. The fast particles are thus accelerated either directly or stochastically, and could produce the FTSs (Priest 1981).

4 DISCUSSION

4.1 Other Probable Origins of the Homologous Radio Bursts

It is also probable that a disruption of the large-scale coronal magnetic field permits the electron acceleration and energy release in a flare, and a flare at a remote location could occur at where the field lines are disrupted by the passage of the flux tube (Kundu et al. 2004). Another possibility which cannot be ruled out is the energy release due to spontaneous, propagating reconnection which allows the system essentially to brighten locally (de La Beaujardiere et al. 1995). Moreover, the energy for the homologous flares/bursts driven by the post-flare loops may be obtained from the solar wind, which drags field lines upward into an open configuration, resulting in the later magnetic reconnection that produces the late phase homologous flares corresponding to the radio bursts (Pneuman 1981).

4.2 Reasons for the Rarity of Homologous Radio Bursts

We should stress that not all evolving fluxes are capable of producing homologous flares/bursts in post-flare loops. Homologous flares/bursts are triggered only if they contain sufficient stored energy, and they also need the large-scale field to be strong sheared (Priest 1981). In addition, the case may be similar to the visibility of the coronal transient brightenings, which involve the physical conditions in the loops, such as the plasma density, temperature and magnetic pressure (Shimizu et al. 1994). If we propose that the energy for homologous flares/bursts is derived from the solar wind which drags the field lines of the post-flare loops outward into a quasi-open configuration, then this energy could only be released occasionally to produce homologous flares/bursts (Pneuman 1981).

5 SUMMARY

The main properties of these homologous radio bursts are: they consist of a broad-band complex microwave radio burst in the early phase and a narrow-band decimetric burst in the late phase, as well as radio FTSs (i.e., normally and reversely drifting type III bursts with slowly or no drifting structures). Unipolar, bipolar, tripolar and quadrupolar magnetic structures of radio sources are found during these bursts. Our analyses confirm that the main single-bipole magnetic structure produced by newly and/or repeatedly, appearing or disappearing magnetic polarity of radio source causes a two-ribbon flare (corresponding to broad-band microwave burst) and later, a homologous burst (corresponding to the narrow-band decimetric burst). Various radio FTSs could be related to the multipole (tripole or quadrupole) magnetic structures.

Our observations support the ‘Y-type’ model with single-bipole structure, and the ‘multiloop’ model with tripolar or quadrupolar structures (i.e., a unified model of plasmoid-induced-reconnection, which includes the CSHKP and the emerging flux model, see Shibata 1999). The ‘Y-type’ model could cause radio bursts of long duration (i.e., early broad-band microwave and later narrow-band decimetric homologous radio bursts), while the ‘multiloop’ model could cause the radio emissions of FTSs.

Acknowledgements We thank the research group in NAOC, Beijing, for providing radio data. This research is supported by the National Natural Science Foundation of China (Grants 19833050, 19973016, 10333030 and 10473020), the “973” project (No. 2006CB806300), and the Project of Cultivating Western Talents of the Chinese Academy of Sciences.

References

- Aschwanden M. J., Kosugi T., Hanaoka Y. et al., 1999, *ApJ*, 526, 1026
- Aschwanden M. J., 2002, *Space Science Reviews*, 101/1-2, 1, Dordrecht: Kluwer Academic Publishers
- Carmichael H., 1964, in *AAS-NASA Symp on the Physics of Solar Flares*, W. N. Hess, ed., NASA-SP 50, p.451
- Démoulin P., van Driel-Gesztelyi L., Schmieder B. et al., 1993, *A&A*, 271, 292
- de La Beaujardière J.-F., Canfield R. C., Hudson H. S. et al., 1995, *ApJ*, 440, 386
- Fu Q. J., Li C. S., Jin S. Z., 1985, In: C. deJager, B. Chen eds., *Proc. of Kunming Workshop on Solar Physics and Interplanetary Travelling Phenomena*, Beijing: Science Press, p.560
- Gopalswamy N., Zhang J., Kundu M. R. et al., 1997, *ApJ*, 491, L115
- Green L. M., Matthews S. A., van Driel-Gesztelyi L. et al., 2002, *Solar Phys.*, 205, 325
- Hanaoka Y., 1994, *ApJ*, 420, L37
- Hanaoka Y., 1997, *Solar Phys.*, 173, 319
- Heyvaerts J., Priest E. R., Rust D. M., 1977, *ApJ*, 216, 123
- Hirayama T., 1974, *Solar Phys.*, 34, 323
- Hudson H., Fletcher L., Khan J. I. et al., 2004, in D. E. Gary, C. U. Kellerr, eds., *Solar and Space Weather Radiophysics*, Chapter 8, p.153
- Ji H. R., Fu Q. J., Lao D. B., 1997, *Acta Astrophys. Sinica*, 17, 219
- Ji H. R., Fu Q. J., Liu Y. Y., 2000, *Acta Astrophys. Sinica*, 20, 209
- Kopp R. A., Pneuman G. W., 1976, *Solar Phys*, 50, 85
- Kundu M. R., 1983, *Solar Phys.*, 86, 205
- Kundu M. R., White S. M., Garaimov V. I. et al., 2004, *ApJ*, 607, 530
- Machado M. E., Moore R. L., Hernandez A. M. et al., 1998, *ApJ*, 326, 425
- Mandrini C. H., Démoulin P., Hénoux J. C. et al., 1991, *A&A*, 250, 541
- Martens P. C. H., Kuin N. P. M., 1989, *Solar Phys.*, 122, 263
- Martres M. J., 1989, *Solar Phys.*, 119, 357
- Masuda S., Kosugi T., Hara H. et al., 1994, *Nature*, 371, 495
- Masuda S., Kosugi T., Hara H. et al., 1995, *Publ. Astron. Soc. Japan*, 47, 677
- Moore R. L., McKenzie D. L., Svestka Z. et al., 1980 in *Solar Flares*, P. Sturrock, ed., Chapter 7, Col. Ass. Uni. Press
- Nakajima H. et al., 1994, *Proc. IEEE*, 82, 705
- Nishio M., Yaji K., Kosugi T. et al., 1997, *ApJ*, 489, 976
- Parker E. N., 1988, *ApJ*, 330, 474
- Petschek H. E., 1964, in *AAS-NASA Symp on the Physics of Solar Flares*, W. N. Hess, ed., NASA-SP 50, p.425
- Pneuman G. W., 1981, in *Solar Flare Magnetohydrodynamics*, E. R. Priest, ed., New York: Gordon and Breach, p.379
- Priest E. R., 1981, in *Solar Flare Magnetohydrodynamics*, E. R. Priest, ed., New York: Gordon and Breach, p.139
- Priest E. R., Forbes T. G., 2002, *Astro. Ap. Revs.*, 10, 313
- Ranns N. D. R., Harra L. K., Matthews S. A. et al., 2000, *A&A*, 360, 1163
- Sakai J.-I., De Jager C., 1991, *Solar Phys.*, 134, 329
- Shibata K., 1999, *Ap&SS*, 264, 129
- Shimizu T., Tsuneta S., Acton L. W. et al., 1994, *ApJ*, 422, 906
- Sturrock P. A., 1966, *Nature*, 211, 695
- Sui L., Holman G. D., Dennis B. R., 2004, *ApJ*, 612, 546
- Tajima T., Sakai J., Nakajima H. et al., 1987, *ApJ*, 321, 1031
- Takakura T., Scalise E. Jr., 1970, *Solar Phys.*, 11, 434
- Wang M., Xie R. X., Xu C. et al., 2005, *Chin. J. Astron. Astrophys. (ChJAA)*, 5, 508
- Woodgate B. E., Martres M. -J., Smith J. B. et al., 1984, *Advances in Space Physics Research*, 4, 11
- Zhang J., Wang J., 2002, *ApJ*, 566, L117